# CHAPTER IV

DEPOSITION MATHEMATICAL EXPLANATION

4.1 Deposition Governing Equations

In order to predict wax deposition and to gain a better understanding of wax deposition, mass and energy balances need to be developed for the coldfinger. Singh *et al.* (2000) have developed mass and energy balances for the flow loop, but these equations can not be directly applied for coldfinger system because the flow loop geometry differs from coldfinger. In the flow loop system, liquid flows horizontally and the temperature drops in both the radial and axial directions. However, in the coldfinger system, liquid circulates around the coldfinger and its temperature drops from the bulk to the coldfinger probe in a radial direction. Due to these differences, heat and mass transfer coefficients for the coldfinger also differ from the flow loop and can not be obtained by the same empirical correlation. This section will take Singh's equations and modify them for the coldfinger in a cylindrical coordinate system as shown in Figure 4.1.
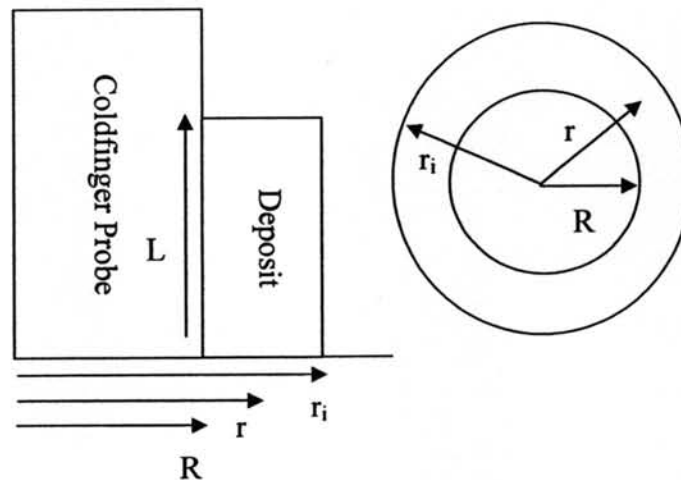
Figure 4.1 Coldfinger coordinate system.

All notations for the equations are provided in Appendix B. The deposition mechanism suggested by Singh is that wax molecules in the bulk convectively flow to the fluid-deposit interface and then diffuse into the deposit and precipitate,

changing the deposit composition. Therefore, the mass balance on a depositing species is

| Rate of change of species j in the deposit | = | Radial convective flux of species j molecules form the bulk to the fluid- deposit interface |

The rate of change of species j in the deposit is

$$\frac{dm_j}{dt} = \frac{d}{dt}\int_{V_g} F_j(t,r)\rho_{gel}(F_j, F_{j+1},...)dV_g \qquad (4.1)$$

As suggested by Singh, the density of gel, ρ_{gel} is constant through the deposit because oil density and wax density are approximately the same on a mass basis as shown in Table 4.1.

Table 4.1 Density of liquid n-alkanes at 25°C (Haulait-Pirson *et al.*, 1987)

Species	Density (ρ)	
	mol/m^3	kg/m^3
C_{12}	4374	744
C_{28}	2039	803
C_{32}	1799	809
C_{36}	1610	814

Thus,
$$\frac{dm_j}{dt} = \frac{d}{dt}\rho_{gel}\int_{V_g} F_j(t,r)dV_g \qquad (4.2)$$

For a thin deposit, solid wax fraction in the deposit is independent of position in the deposit as shown by the result of Singh (Singh *et al.*, 2001). Hence, $\frac{dm_j}{dt}$ becomes

$$\frac{dm_j}{dt} = \frac{d}{dt}\rho_{gel}\overline{F}_j(t)\int_{V_g} dV_g = \frac{d}{dt}\rho_{gel}\overline{F}_j(t)\int_0^L\int_0^{2\pi}\int_R^{r_i} rdrd\theta dz \qquad (4.3)$$

$$\frac{dm_j}{dt} = \frac{d}{dt}\left[\rho_{gel}\overline{F}_j(t)\pi\left(r_i^2 - R^2\right)L\right] \qquad (4.4)$$

where
$$\overline{F}_j = \frac{\int\limits_{V_g} F_j(t)dV_g}{\int\limits_{V_g} dV_g} \qquad (4.5)$$

By equating the $\dfrac{dm_j}{dt}$ term in Equation 4.4 with the radial convective flux term, dependent on the concentration gradient between the bulk fluid and the deposit interface, the mass balance equation becomes

$$\frac{d}{dt}\left[\pi\left(r_i^2 - R^2\right)L\overline{F}_j(t)\rho_{gel}\right] = 2\pi r_i k_{lj}\left[C_{jb} - C_{ji}(T_i)\right] \qquad (4.6)$$

By using the chain rule, Equation 4.6 becomes

$$\rho_{gel}\pi L\left(r_i^2 - R^2\right)\frac{d\overline{F}_j(t)}{dt} + 2\pi L\rho_{gel}\overline{F}_j(t)r_i\frac{dr_i}{dt} = 2\pi L r_i k_{lj}\left[C_{jb} - C_{ji}(T_i)\right] \qquad (4.7)$$

From the deposition mechanism, wax molecules will be transferred from the bulk to the deposit and diffuse into the deposit. Hence, the deposit growth balance will be

Rate of addition of	=	Radial convective flux of	-	Diffusive flux of
species j in growing		wax molecules from the bulk		species j into the gel
the gel deposit		to the fluid-gel interface		at the deposit interface

$$2\pi r_i \overline{F}_j(t)\rho_{gel}L\frac{dr_i}{dt} = 2\pi r_i k_{lj}L\left[C_{jb} - C_{ji}(T_i)\right] - 2\pi r_i L\left[D_{ejg}\frac{dC_{jg}}{dr}\right]_i \qquad (4.8)$$

where the subscript g denotes the gel side. Solving for $\dfrac{dr_i}{dt}$ yields

$$\frac{dr_i}{dt} = \frac{k_{lj}\left[C_{jb} - C_{ji}(T_i)\right] - \left[D_{ejg}\dfrac{dC_{jg}}{dT}\dfrac{dT_g}{dr}\right]_i}{\overline{F}_j(t)\rho_{gel}} \qquad (4.9)$$

where
$$\left.\frac{dC_{jg}}{dr}\right|_i = \left[\frac{dC_{jg}}{dT}\frac{dT_g}{dr}\right]_i \qquad (4.10)$$

The effective diffusivity, D_{ejg}, can be estimated using the following expression developed by Cussler derived for porous media of flake-like particles as suggested by Singh (Cussler *et al.*, 1988; Singh *et al.*, 2000).

$$D_{ejg} = \frac{D_{jog}}{1 + \alpha^2 \overline{F}_w^2 / (1 - \overline{F}_w)}$$ (4.11)

where $$\alpha = 1 + \alpha_c \overline{F}_w$$ (4.12)

α is assumed to increase linearly with total wax fraction as suggested in Singh's work (Singh *et al.*, 2000). α_c is an unknown constant that can be found by fitting the deposition model with experimental results. The change in composition of component j in the deposit over time can be found by subtracting Equation 4.8 from Equation 4.7.

$$\frac{d\overline{F}_j(t)}{dt} = \frac{2r_i D_{ejg} \left.\dfrac{dC_{jg}}{dr}\right|_i}{\rho_{gel}(r_i^2 - R^2)} = \frac{2r_i \left[D_{ejg} \dfrac{dC_{jg}}{dT} \dfrac{dT_g}{dr} \right]_i}{\rho_{gel}(r_i^2 - R^2)}$$ (4.13)

Equations 4.11 and 4.13 show that for a coldfinger system, the rate of change of deposit wax fraction is dependent on its effective diffusivity, solubility at the interface, and crystal aspect ratio in the deposit. When F_j increases, $\dfrac{dF_j}{dt}$ will decrease because of a decrease in D_{ej}.

Equations 4.7 and 4.8 have many unknown variables. However, all of these variables can be written as a function of one of three variables: T_i, r_i, and F_j. For example, α can be assumed to be a linear function of F_j as suggested by Singh and C_{js} is a function of T_i. In order to have a solvable set of equations, one more equation relating the three core variables to one another is necessary. By completing an energy balance, the third equation is obtained. In the energy balance, heat entering the deposit comes from convective heat from the bulk fluid and the heat released from the wax solidification process. Thus,

Radial convective heat flux = Rate of heat conduction - Heat generation

from the bulk to the interface   through the deposit   from solidification

$$2\pi r_i L h(T_b - T_i) = \frac{2\pi L k_e (T_i - T_a)}{\ln\left(\frac{r_i}{R}\right)} - \sum_j \left[2\pi r_i L \left(\rho_{gel}\overline{F}_j(t) - C_{ji}(T_i)\right)\frac{dr_i}{dt}\Delta H_j\right]$$

(4.14)

Substituting Equation 4.9 into Equation 4.14 yields

$$r_i h(T_b - T_i) = \frac{k_e (T_i - T_a)}{\ln\left(\frac{r_i}{R}\right)} - \sum_j \left[r_i\left(1 - \frac{C_{ji}(T_i)}{\rho_{gel}\overline{F}_j(t)}\right)\left(k_{lj}\left[C_{jb} - C_{ji}(T_i)\right] - \left[D_{ejg}\frac{dC_{jg}}{dT}\frac{dT_g}{dr}\right]_i\right)\Delta H_j\right]$$

(4.15)

Rearranging Equation 4.15 allows for the development of a relationship to calculate T_i.

$$T_i = \frac{T_b r_i h \ln\left(\frac{r_i}{R}\right) + k_e T_a + \sum_j \left[r_i \ln\left(\frac{r_i}{R}\right)\left(1 - \frac{C_{ji}(T_i)}{\rho_{gel}\overline{F}_j(t)}\right)\left(k_{lj}\left[C_{jb} - C_{ji}(T_i)\right] - \left[D_{ejg}\frac{dC_{jg}}{dT}\frac{dT_g}{dr}\right]_i\right)\Delta H_j\right]}{k_e + r_i h \ln\left(\frac{r_i}{R}\right)}$$

(4.16)

where $\qquad k_e = \frac{\left[2k_w + k_{oil} + (k_w - k_{oil})F_w\right]}{\left[2k_w + k_{oil} - 2(k_w - k_{oil})F_w\right]}k_{oil}$ (4.17)

To estimate T_i, the third term in Equation 4.16 will be neglected because it is relatively small compared to first two terms. k_{li} in Equation 4.16 will be estimated to show how important the third term in Equation 4.16 is by assuming that the Sherwood number (Sh) equals the Nusselt number (Nu). When Sh equals Nu, $\frac{k_{lj}L_{char}}{D_{jo}} = \frac{hL_{char}}{k_{oil}}$, then $k_{lj} = \frac{D_{jo}h}{k_{oil}}$. h is a value that can be determined experimentally.

In order to estimate the convective heat transfer coefficient at the conditions used in this work, pure dodecane was used because dodecane is the primary species in the bulk fluid. Initially, the dodecane temperature was held at room temperature in order to minimize heat loss to the surroundings. Then, the coldfinger probe was immersed into the system and the liquid temperature was measured. By using the

first law of thermodynamics and neglecting the shaft work from the stirrer to the system, the heat transfer from the bulk liquid into the coldfinger probe in an interval time dt must equal to the decrease in internal energy of the liquid.

$$hA(T - T_a)dt = -c_p\rho V dT$$

$$\int_{T_{bo}}^{T} \frac{dT}{T - T_a} = -\frac{hA}{c_p\rho V} \int_{0}^{t} dt$$

$$\ln\left(\frac{T - T_a}{T_{b0} - T_a}\right) = -\frac{Aht}{\rho V c_p}$$

$$\ln(T - T_a) = -\frac{Aht}{\rho V c_p} + \ln(T_{ini} - T_a) \qquad (4.18)$$

Equation 4.18 can be used to find h experimentally by plotting $\ln(T-T_a)$ as a function of t. The slope and the intercept of the graph will be $-\dfrac{Ah}{\rho V c_p}$ and $\ln(T_{b0}-T_a)$ respectively. The result of this experiment can be seen in Figure 4.2.

To determine h from Figure 4.1, c_p was used at 20°C, which is 372.74 J/(mol·°K) (González-Salgado et al., 2004), the mass of dodecane (ρV) used was 149.58 g, and the coldfinger contacted surface area was 7.9 cm^2. h was estimated to be 235.1 W/(m^2·°K).

y = -5.676E-04x + 2.505
R^2 = 0.973
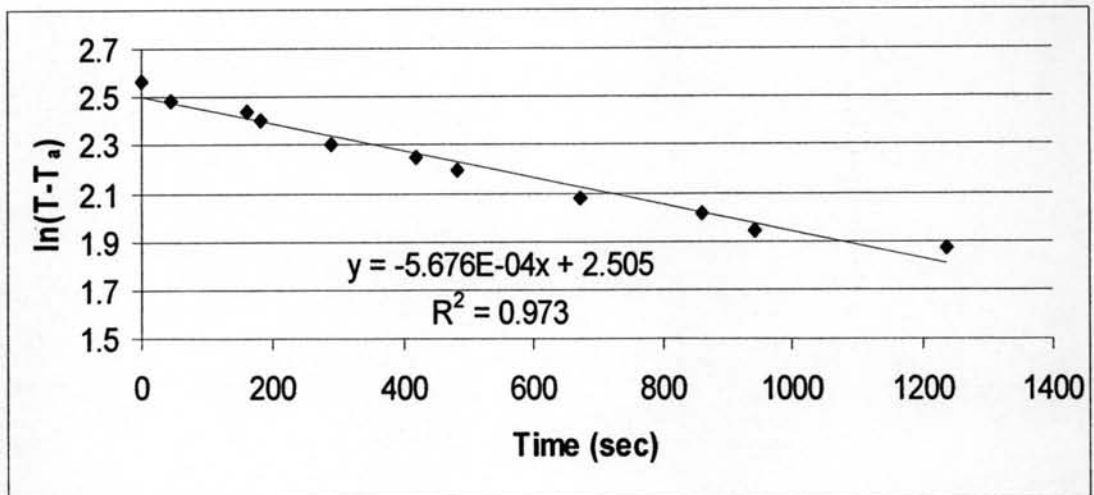
Figure 4.2 Temperature change as a function of time to estimate h.

This value of h is used to evaluate the third term of Equation 4.16 and its magnitude can be compared to the other terms. The evaluation of Equation 4.16 for a 4% C_{36} system can be seen in Table 4.2.

Table 4.2 Evaluation of the third term in Equation 4.16 of C_{36} system

Variable	Relation	Value
C_{36} molecular diffusivity in dodecane at 50°C, D_{C36o}		$7.07 \times 10^{-10}\,\mathrm{m^2/s}$
k_{oil} assumed to be k_{C12} at 50°C		$0.131\ \mathrm{W\,m^{-1}K^{-1}}$
r_{iC36}		0.61 cm
Mass transfer coefficient, k_{lj}	$k_{li} = \dfrac{D_{io}h}{k_{oil}}$	1.3×10^{-6} m/s
First term in Equation 4.16	$T_b r_i h \ln\left(\dfrac{r_i}{R}\right) \Big/ \left(k_e + r_i h \ln\left(\dfrac{r_i}{R}\right)\right)$	34.3°C
Second term in Equation 4.16	$k_e T_a \Big/ \left(k_e + r_i h \ln\left(\dfrac{r_i}{R}\right)\right)$	1.5°C
Third term in Equation 4.16	$\dfrac{r_i \ln\left(\dfrac{r_i}{R}\right)\sum_i k_{li}\left[C_{jb} - C_{js}(T_i)\right]\Delta H_j}{k_e + r_i h \ln\left(\dfrac{r_i}{R}\right)}$	0.08°C

Values of k_{C12}, D_{C36o}, and r_{iC36} in Table 4.2 come from works of Burgdorf, Hayduk and Haulait-Pirson, and data in Chapter 4 respectively (Burgdorf *et al.*, 1999; Hayduk and Minhas, 1982; Haulait-Pirson, *et al.*, 1987). D_{ejg}, $\left(1 - \dfrac{C_{ji}(T_i)}{\rho_{gel}\overline{F}_j(t)}\right)$ and $[C_{jb} - C_{js}(T_i)]$ are estimated to equal 0, 1 and C_{jb} respectively to maximize the value of the third term in Equation 4.16. Table 4.2 shows the third term in Equation 4.16 is negligible in comparison to the first two terms. Even if the assumption that Sh = Nu is not completely valid and k_{lj} were a factor of 10 higher, the third term would

still be small, 0.8°C. In this work, the value of the third term for the polydisperse system will also be neglected.